JOURNAL OF AGRICULTURAL AND FOOD CHEMISTRY

Article

pubs.acs.org/JAFC

$CoFe_2O_4$ Nanoparticles as Oxidase Mimic-Mediated Chemiluminescence of Aqueous Luminol for Sulfite in White Wines

Xiaodan Zhang,[†] Shaohui He,[†] Zhaohui Chen,*[,†,‡] and Yuming Huang*[,†]

[†]The Key Laboratory of Luminescence and Real-time Analysis, Ministry of Education, College of Chemistry and Chemical Engineering, Southwest University, Chongqing 400715, China

[‡]Basic Department of Rongchang Campus, Southwest University, Chongqing 402460, China

Supporting Information

ABSTRACT: Recently, the intrinsic enzyme-like activity of nanoparticles (NPs) has become a growing area of interest. However, the analytical applications of the NP-based enzyme mimetic are mainly concentrated on their peroxidase-like activity; no attempts have been made to investigate the analytical applications based on the oxidase mimic activities of NPs. For the first time, we report that $CoFe_2O_4$ NPs were found to possess intrinsic oxidase-like activity and could catalyze luminol oxidation by dissolved oxygen to produce intensified chemiluminescence (CL). The effect of sulfite on $CoFe_2O_4$ NP oxidase mimic-mediated CL of aqueous luminol was investigated. It is very interesting that when adding sulfite to the luminol−$CoFe_2O_4$ system, the role of sulfite in the luminol−$CoFe_2O_4$ NP−sulfite system depends on its concentration. At a relatively low concentration level, sulfite presents an inhibition effect on the luminol−$CoFe_2O_4$ NP system. However, it does have an enhancement effect at a higher concentration level. Investigations on the effect of the solution pH and luminol and $CoFe_2O_4$ NP concentrations on the kinetic characteristics of the studied CL system in the presence of trace sulfite suggested that the enhancement and inhibition of the luminol−$CoFe_2O_4$ NP−sulfite CL system also depended on the solution pH. It seems that the concentrations of luminol and $CoFe_2O_4$ NPs did not influence the CL pathway. The possible mechanism of the luminol−$CoFe_2O_4$ NP−sulfite CL system was also discussed. On this basis, a flow injection chemiluminescence method was established for the determination of trace sulfite in this study. Under the optimal conditions, the proposed system could respond down to 2.0×10^{-8} M sulfite. The method has been applied to the determination of trace sulfite in white wine samples with satisfactory results. The results given by the proposed method are in good agreement with those given by the standard titration method.

KEYWORDS: *oxidase mimic, $CoFe_2O_4$ nanoparticles, chemiluminescence, food analysis, sulfite, white wine*

INTRODUCTION

Sulfite has attracted much attention since its common use as a preservative in food, wine, and drugs to prevent oxidation, inhibit bacterial growth, and control enzymatic and nonenzymatic reactions with stabilizing and conditioning functions.[1] However, the sulfite level in various products is strictly limited because accumulating evidence has suggested that sulfite compounds cause toxic and adverse effects on mammals.[2−5] Also, it was discovered that a high concentration level of sulfite causes asthmatic attacks and allergic reactions in some individuals.[6] On this basis, the U.S. Food and Drug Administration (FDA) has required labeling of products containing more than 10 μg mL^{-1} sulfite in food or beverages since 1986.[7] Therefore, the determination of sulfite is important particularly from biological and industrial points of view.

To realize the analysis of trace sulfite, various methods such as chromatographic,[8,9] amperometric,[10−12] biosensor,[13] spectrophotometric,[14] and CL[15−19] methods have been developed. CL methods promise ultrasensitive detection limits (attomole to zeptomole), rapid assays, and a broad range of analytical applications with simple instruments (no monochromator required). However, the study of CL was limited to some molecular systems.[20−22] Recently, with the development of nanotechnology, nanoparticles (NPs) have been applied in CL systems.[23−32] Among these systems, some NPs have been used as reductants, catalysts, and luminophores in the aqueous phase. For instance, Cui and co-workers have found that gold NPs with 5 and 6 nm in diameter that received energy from an energy-rich intermediate of 1,2-dioxetanedione produced from bis(2,4,6-trichlorophenyl) oxalate oxidized by hydrogen peroxide could lead to CL emission (gold NPs were identified as the emitting species).[25] In addition, they have demonstrated that gold NPs could be used as an effective catalyst for catalyzing the reaction of H_2O_2 and luminol.[26] For another example, gold NPs as reductant could reduce potassium permanganate in a strong acid medium to the excited state of Mn(II), resulting in light emission.[27] Besides the above-mentioned examples, NPs have also been investigated for nanolabels of immunoassay[28] and gas sensors for sensing of various gases such as ethanol, acetone, and chlorinated volatile organic compounds in gas-phase CL analysis.[23,24,33,34] More recently, Li's group has found that CdTe QDs, as a kind of sensitizer, could enhance the CL emission from the redox reaction of SO_3^{2-} with Ce(IV) in acidic medium.[19] All these achievements provide new insights into the potential applications of NPs in bioanalysis, environmental analysis, and labeling probes.[23,24,28,33,34]

Received: September 26, 2012
Revised: December 3, 2012
Accepted: January 4, 2013
Published: January 5, 2013

Recently, along with the interesting and important finding that the Fe_3O_4 NPs possess unique artificial peroxidase activity, more and more NPs have been evaluated as enzymatic mimetics, including ferromagnetic NPs[35−40] and V_2O_5 nanowires[41] as peroxidase mimetics, ceria oxide NPs as oxidase mimetic,[42−44] and metal NPs[45−49] and carbon-based nanomaterials[50−55] as oxidase or peroxidase mimetics. The intrinsic enzyme-like activity of nanomaterials has become a growing area of interest, which has been summarized in a recent review.[56] However, almost all of the analytical applications of the NP-based enzyme mimetics are based on their peroxidase-like activities; no attempts have been made to investigate the analytical applications based on the oxidase mimic activities of NPs. Furthermore, almost all of the reported NP-based enzyme mimetics have been based on a colorimetric method to date. There is limited study documenting the CL-based method for screening of the NP-based enzyme mimetics.[38] Here, for the first time, we report that $CoFe_2O_4$ NPs as oxidase mimic could catalyze luminol oxidation by dissolved oxygen to produce intensified CL. It is very interesting that when adding sulfite to the luminol−$CoFe_2O_4$ NP system, the role of sulfite in the studied CL system depends on its concentration. At a relatively low concentration level, sulfite presents an inhibition effect on the luminol−$CoFe_2O_4$ NP CL system. However, it does have an enhancement effect at a higher concentration level. Further study suggested that the CL enhancement and inhibition of luminol−$CoFe_2O_4$ NP−sulfite also depended on the solution pH. On the basis of the above finding, we investigated the kinetic characteristics of the studied CL system affected by the solution pH and luminol and $CoFe_2O_4$ concentrations in the presence of different sulfite concentration levels. Finally, a flow injection CL method was established for the determination of trace sulfite in this study. The developed method was applied to the determination of sulfite in white wines, and the results were compared with those by the conventional titration method in the interest of demonstrating the feasibility and reliability of the proposed method.

EXPERIMENTAL PROCEDURES

Reagents and Chemicals. All chemicals used in this work were of analytical grade and were used as received without further purification. *o*-Phenylenediamine (OPD), 2,2′-azinobis(3-ethylbenzothiazoline-6-sulfonic acid) diammonium salt (ABTS), and 3,3,5,5-tetramethylbenzidine (TMB) were purchased from Sigma-Aldrich (St. Louis, MO) and stored in a refrigerator at 4 °C. Luminol was from Merck (Germany); a 0.01 M luminol solution was prepared in 1000 mL of 0.01 M NaOH solution. A sulfite solution was prepared daily by dissolving anhydrous sodium sulfite in water and was standardized by iodimetric titration when needed. All other reagents such as sodium carbonate, sodium hydrogen carbonate, hydrochloric acid, sodium hydroxide, sodium dihydrogen phosphate, ferric chloride, and cobalt nitrate were obtained from the Chongqing Chemical Reagents Co. (Chongqing, China). All glassware was soaked in 10% nitric acid and thoroughly cleaned before use. A 0.1 M Na_2CO_3 solution was used as the basic medium for luminol CL reaction.

Instrumentation. The pH of the solutions was detected by a PHS-3D pH meter (Shanghai Precision Scientific Instruments Co., Ltd., China). CL measurements were performed on an MCFL-A multifunction chemiluminescence/bioluminescence analyzer (Ruike Electronic Equipment Co. Ltd., Xi'an, China). The CL spectra were recorded on an F-7000 spectrofluorimeter (Hitachi, Japan) under a model of the fluorescence scan by turning off the excitation light.

Synthesis of $CoFe_2O_4$ Nanoparticles. The $CoFe_2O_4$ NPs were synthesized via the solvothermal method. The detailed procedure for preparation and the characterization were described in our previous work, and the concentration of the stock solution of the as-prepared $CoFe_2O_4$ NPs was 80.0 g L^{-1}.[38]

General Procedure for CL Analysis. The CL intensity was measured by a flow injection CL system, in which two peristaltic pumps (30 r min^{-1}, Longfang Instrument Factory, Wenzhou, China) were used to deliver all solutions, one at a flow rate of 3 mL min^{-1} (per tube) for delivering the sample solution and water carrier stream and the other for delivering luminol and $CoFe_2O_4$ NP solutions at a flow rate of 3 mL min^{-1} (per tube). Poly(tetrafluoroethylene) (PTFE) tubing (0.8 mm i.d.) was used to connect all components in the flow system. For CL measurement, flow lines were inserted into the luminol solution, water, and $CoFe_2O_4$ NP solution. Then the pumps were started until a stable baseline was recorded. Injection was made by using an eight-way injection valve equipped with a 200 μL sample loop. The CL signal was recorded by a computer equipped with a data acquisition interface. Data acquisition and processing were performed with REMAX software running under Windows XP. For characterization of the chemiluminescent analysis system, aqueous standards were used. A series of working standard solutions with different concentrations were prepared by diluting a concentrated fresh standard solution of sulfite with water. The net CL emission intensity ($\Delta I = I_1 - I_0$, where I_1 is the CL intensity of the sample solution and I_0 that of the blank solution) versus sulfite concentration was used for the calibration. At each sulfite concentration, the injection was repeated at least three times, and the average CL signal was obtained.

Procedure for White Wine Samples. Four white wine samples were analyzed by the proposed method. For this purpose, 25 mL of each of the selected white wine samples was added into a glass baker, heated until the remaining solution in the baker was about 10 mL, transferred to a 25 mL volumetric flask, and then diluted with distilled water for analysis.

Comparison Study between the Proposed Method and the Standard Method. When the comparison study was performed, the sulfite analysis was carried out according to the method given in the State Standard of the People's Republic of China.[57] Briefly, after 5 mL of white wine sample, 50 mL of water, and 10 mL of 1:1 HCl were added to a 100 mL volumetric flask, the mixture was boiled until the remaining solution in the flask was about 10 mL, and any sulfur dioxide was then driven over into the cooled receiver containing 25 mL of 20 g L^{-1} $Pb(Ac)_2$ solution as the absorbent solution. The collected solution was acidified by adding 10 mL of the concentrated HCl and then titrated with 1 mM iodine solution using 1 mL of 1% starch as the indicator.

RESULTS AND DISCUSSION

Oxidase-like Activity of $CoFe_2O_4$ NPs and Characteristics of $CoFe_2O_4$ NPs in Oxidase Mimic-Mediated CL of Luminol in the Presence of Sulfite. The oxidase-like activity of $CoFe_2O_4$ NPs was evaluated in the catalysis of the typical substrates TMB, OPD, and ABTS in the absence of H_2O_2. As can be seen, $CoFe_2O_4$ NPs could catalyze the oxidation of TMB, OPD, and ABTS by dissolved O_2 in NaAc buffer and produce the typical color reaction (Figure 1A). Similar to other enzyme mimic reactions, the typical absorbance peak of the oxidation products of TMB is located at 652 nm.[35,44,45,50] The absorbance of the oxidized product of TMB at 652 nm was significantly increased in the presence of $CoFe_2O_4$ NPs (Figure 1B). These results confirm the oxidase-like activity of $CoFe_2O_4$ NPs toward TMB, OPD, and ABTS. The oxidase-like activity of $CoFe_2O_4$ NPs was also evaluated by their catalytic oxidation of luminol by dissolved O_2. Figure 2 shows the CL spectra of the studied luminol CL system in the presence of $CoFe_2O_4$ NPs. As can be seen, luminol can be oxidized by dissolved oxygen to produce a weak light emission, which can be greatly enhanced by $CoFe_2O_4$ NPs with one peak situated at about 430 nm (same as the maximum emission spectrum of 3-aminophthalate), indicating that the role of $CoFe_2O_4$ NPs is only

dx.doi.org/10.1021/jf3041269 | J. Agric. Food Chem. 2013, 61, 840−847

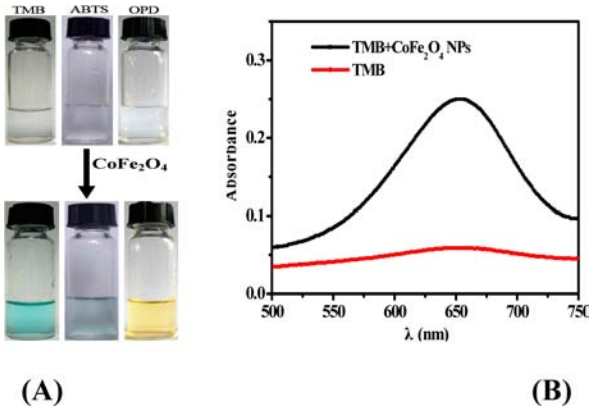

Figure 1. (A) Images of the oxidation color reaction of TMB, ABTS, and OPD by dissolved O_2 with $CoFe_2O_4$ NPs. (B) UV/vis spectra of TMB solution in 0.2 M NaAc buffer (pH 3.0) at 45 °C. The $CoFe_2O_4$ NPs and TMB concentrations were 16 μg mL^{-1} and 0.5 mM, respectively.

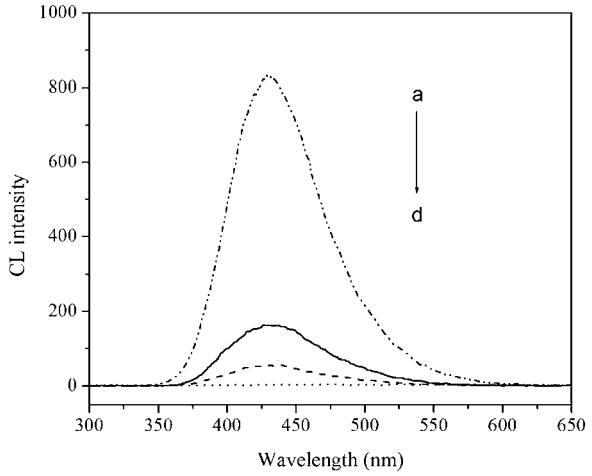

Figure 2. CL spectra of the studied luminol CL system (luminol concentration 10 μM in 0.1 M Na_2CO_3 (pH 11.2), $CoFe_2O_4$ concentration 80 mg L^{-1}): (a) luminol + $CoFe_2O_4$ + 5.0 mM sulfite, (b) luminol + $CoFe_2O_4$, (c) luminol + $CoFe_2O_4$ + 50 μM sulfite, (d) luminol.

as an enhancement catalytic reagent because there is no new emitter produced in the reaction. This suggests the oxidase-like activity of $CoFe_2O_4$ NPs to catalyze the reaction between luminol and dissolved O_2.

To study the $CoFe_2O_4$ NPs oxidase mimic-mediated CL of luminol in the presence of sulfite, the CL spectra with different concentrations of sulfite in the above system were studied by F-4500 fluorimetry. The results shown in Figure 2 clearly demonstrate that role of sulfite in the luminol–$CoFe_2O_4$ NP–sulfite system depends on its concentration. At a relatively low concentration level of 50 μM, sulfite presents an inhibition effect on the luminol–$CoFe_2O_4$ NP system. However, it does have an enhancement effect at a higher concentration level of 5 mM. It is interesting that irrespective of the sulfite concentration, the luminophore for the CL system was still the excited-state 3-aminophthalate anions (3-APA*).

Due to the nature of the luminol reaction, which is more favored under basic conditions, the kinetic curves at different basic pH values in the presence of two levels of sulfite concentration at 1.0×10^{-4} and 1.0×10^{-3} M were investigated. As shown in Figure 3, the curves demonstrate one enhancement peak at pH ranging from 10.7 to 13.0 at

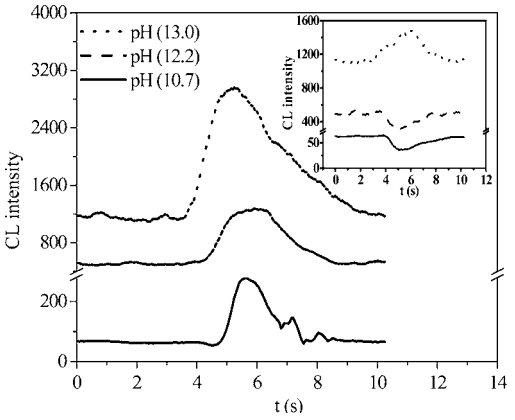

Figure 3. Effect of the luminol pH on kinetic curves (sulfite concentration 1.0 mM, luminol concentration 1.0 μM, $CoFe_2O_4$ NP concentration 8.0 mg L^{-1}). Inset: Effect of the luminol pH on kinetic curves at a sulfite concentration of 0.1 mM.

higher sulfite concentration, whereas at lower sulfite concentration, the curves demonstrate one inhibition peak at pH 10.7 and 12.2 and one enhancement peak at pH 13.0. It seems that the pH of the solutions obviously influenced the CL pathways.

The effect of the sulfite concentration on the CL kinetic curves of the studied CL system was also studied under a pH of 11.2. The experimental results shown in Figure 4 demonstrate

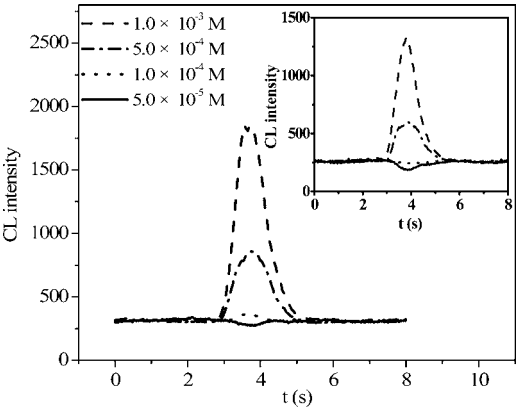

Figure 4. Effect of the sulfite concentration on kinetic curves (luminol concentration 1.0 μM, pH 11.2, $CoFe_2O_4$ NP concentration 8.0 mg L^{-1}). Inset: Effect of the sulfite concentration on kinetic curves after nitrogen purge for 15 min.

that one inhibition peak was observed with 5.0×10^{-5} M sulfite, whereas at relatively higher sulfite concentration (1.0×10^{-4} to 1.0×10^{-3} M sulfite), one enhancement peak was observed. It seems that the sulfite concentration obviously influenced the pathways. It is interesting that, after the solution was purged with nitrogen for about 15 min, the enhancement peak at a sulfite concentration of 1.0×10^{-4} M disappeared and became an inhibition peak (inset in Figure 4), suggesting that dissolved oxygen participated in the CL process, indicating the important role of dissolved oxygen in the CL reaction. The effect of the concentration of $CoFe_2O_4$ NPs on the CL kinetic curves of the system was also studied under a pH of 11.2. The experimental results demonstrate that only one inhibition peak

dx.doi.org/10.1021/jf3041269 | J. Agric. Food Chem. 2013, 61, 840–847

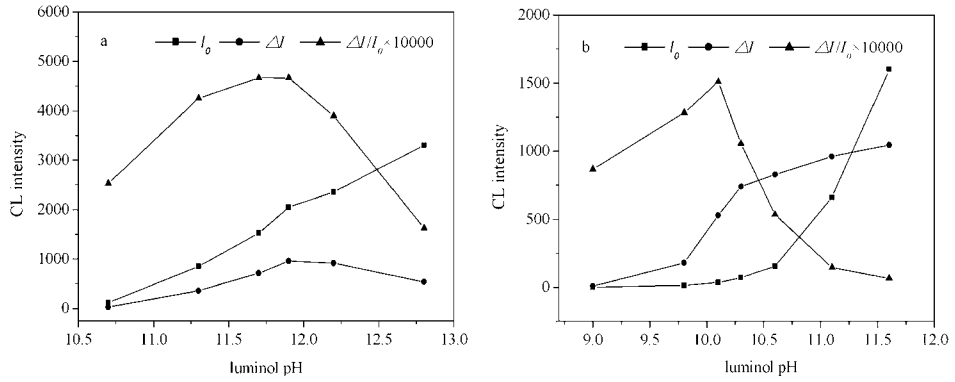

Figure 5. Optimization of the luminol pH: (a) 0.1 mM sulfite, (b) 1.0 mM sulfite (luminol concentration 0.5 μM, $CoFe_2O_4$ NP concentration 8.0 mg L^{-1}).

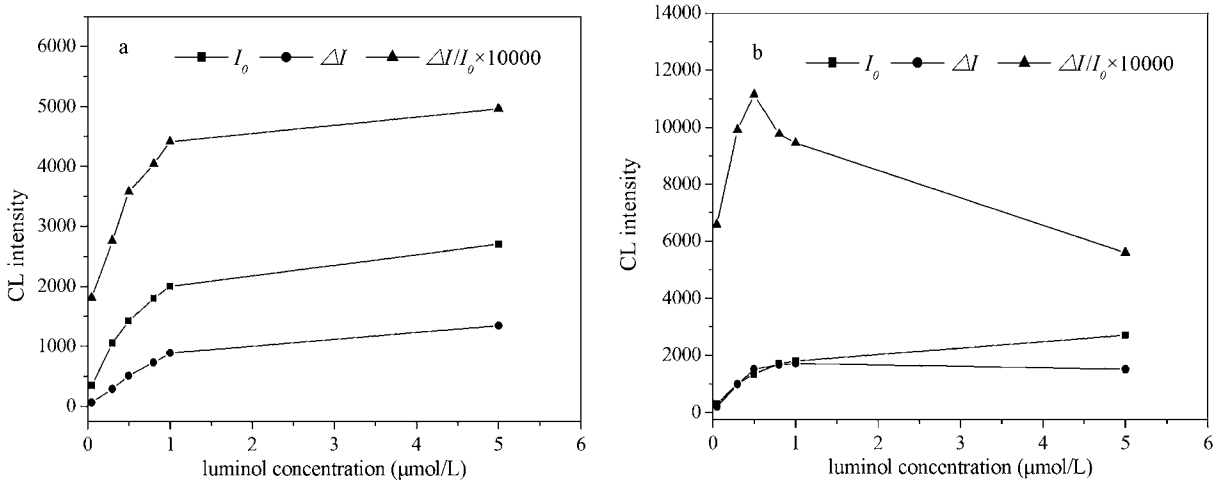

Figure 6. Optimization of the luminol concentration: (a) 0.1 mM sulfite, (b) 1 mM sulfite (pH 11.9, $CoFe_2O_4$ NP concentration 8.0 mg L^{-1}).

was observed with 1.0×10^{-4} M sulfite (Supporting Information, inset in Supplemental Figure S1). However, only one enhancement peak was observed with 1.0×10^{-3} M sulfite (Supporting Information, Supplemental Figure S1). It is possible that the $CoFe_2O_4$ NP concentration did not influence the CL pathway. The effect of the luminol concentration on the CL kinetic curves of the system was studied under a pH of 11.2. The experimental results demonstrate that only one inhibition peak was observed with 1.0×10^{-4} M sulfite (Supporting Information, inset in Supplemental Figure S2). However, only one enhancement peak was observed with 1.0×10^{-3} M sulfite (Supporting Information, Supplemental Figure S2). It is possible that the luminol concentration did not influence the CL pathway. From the above results, it can be concluded that the CL enhancement and inhibition of luminol–$CoFe_2O_4$ NP–sulfite depend on the solution pH and sulfite concentration.

Optimization of the Experimental Conditions. As indicated above, luminol reacts with dissolved oxygen catalyzed by $CoFe_2O_4$ NPs as the oxidase mimic to produce light emission in basic solution. Therefore, the mixture of carbonate and sodium hydroxide as the buffer was added in a flow line to improve the sensitivity of the reaction. The effect of the pH on the CL reaction was studied as shown in the previous section. As can be seen from Figure 5a, in the pH range from 10.7 to 13.0, I_0 increases with an increase of pH; however, in the presence of 1.0×10^{-4} M sulfite, an inhibition CL signal was observed. It was found from Figure 5a that ΔI increased with an increase of pH to 11.8, above which it decreased; however, the background level (I_0) also increased with the pH value. Therefore, the $\Delta I/I_0$ (relative net CL intensity) ratio was used to evaluate the pH effect. As can be seen from Figure 5a, the $\Delta I/I_0$ ratio increases with the pH value to 11.5 and then remains almost stable to pH 12.2, above which the $\Delta I/I_0$ ratio decreases. As a compromise between the sensitivity and the background level, finally, a pH value of 11.9 was selected for the inhibition effect.

Figure 5b depicts the effect of the pH in the presence of 1.0×10^{-3} M sulfite. As can be seen, I_0 increases with an increase of pH from 9.0 to 11.6; however, in the presence of 1.0×10^{-3} M sulfite, an enhancement CL signal was observed. It was found from Figure 5b that ΔI increased with an increase of the pH from 9.0 to 11.6. Considering that the background level (I_0) increases with the pH value, the $\Delta I/I_0$ (relative net CL intensity) ratio was used to evaluate the pH effect. As can be seen from Figure 5b, the $\Delta I/I_0$ ratio increases with the pH value to 10.1; finally, a pH value of 10.1 was selected for the enhancement effect.

The effect of the luminol concentration was investigated from 5.0×10^{-8} to 5.0×10^{-6} M. As can be seen from Figure 6 the effect of the luminol concentration depends on the sulfite concentration. The results shown in Figure 6a indicate that, in the case of an inhibition effect, the $\Delta I/I_0$ ratio sharply increases with the concentration of luminol ranging from 5.0×10^{-8} to 1.0×10^{-6} M and then slowly increases with the concentration

dx.doi.org/10.1021/jf3041269 | J. Agric. Food Chem. 2013, 61, 840–847

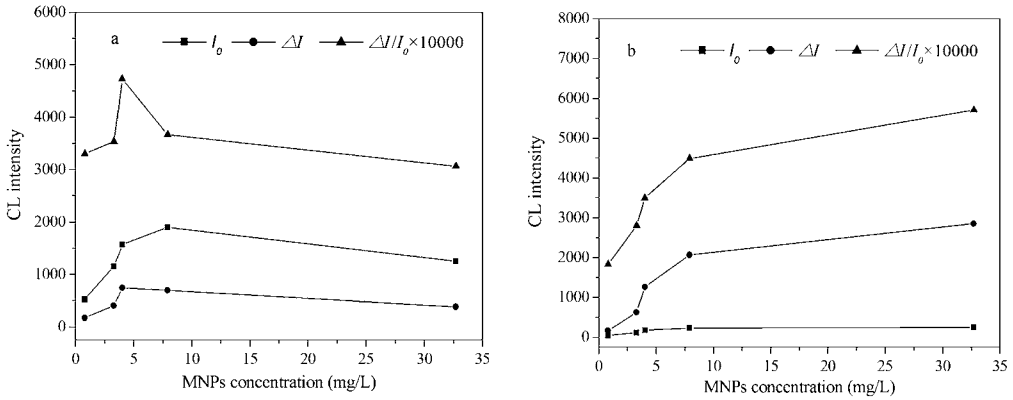

Figure 7. Optimization of the $CoFe_2O_4$ NP concentration: (a) 0.1 mM sulfite, (b) 1 mM sulfite (luminol concentration 10 μM, pH 11.9).

of luminol to 5.0×10^{-6} M. Finally, 1.0×10^{-6} M luminol was used for the inhibition effect in the following work. The experimental results shown in Figure 6b demonstrate that, in the case of an enhancement effect, the $\Delta I/I_0$ ratio increases with the concentration of luminol to 5.0×10^{-7} M, above which the $\Delta I/I_0$ ratio decreases. Therefore, 5.0×10^{-7} M luminol was used for the enhancement effect in the following work.

The effect of the $CoFe_2O_4$ NP concentration on ΔI was investigated ranging from 0.8 to 32.7 mg L^{-1}. Similar to the effect of the luminol concentration, the effect of the NP concentration also depends on the sulfite concentration. The experimental results shown in Figure 7a demonstrate that, in the case of an inhibition effect, the $\Delta I/I_0$ ratio increases with the concentration of $CoFe_2O_4$ NPs to 4.0 mg L^{-1}, above which the $\Delta I/I_0$ ratio decreases. Therefore, 4.0 mg L^{-1} $CoFe_2O_4$ NPs were used for the inhibition effect in the following work. The results shown in Figure 7b indicate that, in the case of an enhancement effect, the $\Delta I/I_0$ ratio sharply increases with the concentration of $CoFe_2O_4$ NPs ranging from 0.8 to 8.0 mg L^{-1} and then slowly increases with the concentration of $CoFe_2O_4$ NPs to 32.7 mg L^{-1}. Therefore, 8.0 mg L^{-1} $CoFe_2O_4$ NPs were used for the enhancement effect in the following work.

In summary, the optimized conditions for the luminol–sulfite–$CoFe_2O_4$ NP-enhanced CL system were as follows: 5.0×10^{-7} M luminol in 0.1 M sodium carbonate and 8.0 mg L^{-1} $CoFe_2O_4$ NPs. The optimized conditions for the luminol–sulfite–$CoFe_2O_4$ NP-inhibited CL system were as follows: 1.0×10^{-6} M luminol in 0.1 M sodium carbonate and 4.0 mg L^{-1} $CoFe_2O_4$ NPs.

Analytical Performance for Sulfite Determination. The possibility of using the proposed method for the determination of sulfite was investigated. The calibration graphs for the determination of sulfite were constructed under the optimum conditions described above. The calibration data of emission intensity versus sulfite concentration are shown in Table 1. As can be seen, the high sensitivity can be realized for sulfite detection with the inhibition mode. In such a case, the detection limit (3σ) for sulfite was 2.0×10^{-8} M. The RSD was 3.4% for 8.0×10^{-6} M sulfite (n = 11).

Table 1. Calibration Range for the Determination of Sulfite

working mode	dynamic range (mM)	regression equation	r^2
inhibition	0.001–0.01	$y = -31801x - 155$	0.9851
enhancement	0.50–4.00	$y = 491.34x - 175$	0.9897

Effect of Foreign Substances. The effect of foreign substances was tested by analyzing a standard solution of sulfite (1.0×10^{-5} M) to which increasing amounts of foreign substances were added. The tolerable concentration ratios with respect to 1.0×10^{-5} M sulfite for interference at the less than 10% level are listed in Table 2. As can be seen, Fe and Cu are the main interferences for sulfite determination. To eliminate the interferences derived from Fe, Cu, and other coexisting transient metals, EDTA was selected as a chelate reagent for the present study. The experimental results indicate that addition of EDTA could realize quantitative recovery of sulfite from samples as compared to those without EDTA addition. Hence, for real sample analysis for sulfite, EDTA was selected for eliminating the possible interferences from metal ions.

Determination of Sulfite in White Wine Samples. As an illustration of analytical application, the proposed method was used to determine total sulfite in white wine samples under the optimal experimental conditions shown above. To eliminate the possible interferences from metal ions, EDTA was used as a masking reagent. The results listed in Table 3 agree well with those obtained by the titration method with iodine.[57]

Possible CL Mechanism. It has been reported that $O_2^{\bullet-}$ and $^{\bullet}OH$ radicals are important intermediates in luminol chemiluminescence.[58,59] To investigate the possible active intermediate in the present CL system, *p*-benzoquinone (BQ) and terephthalic acid (TPA) were selected for the purpose because it has been reported that *p*-benzoquinone is a good trapper for $O_2^{\bullet-}$ [60,61] and terephthalic acid (TPA) can react with $^{\bullet}OH$.[62] The results suggested that, whether in the case of enhancement or inhibition, the CL intensity was completely inhibited in the presence of BQ; however, it was only partially suppressed in the presence of TPA (Supporting Information, Supplemental Figures S3 and S4). This evidence demonstrates that although $O_2^{\bullet-}$ and $^{\bullet}OH$ radicals are formed in the $CoFe_2O_4$ NP-participating catalytic reaction, $O_2^{\bullet-}$ radical is probably the main reactive intermediate. The produced $O_2^{\bullet-}$ and $^{\bullet}OH$ radicals react with luminol, yielding an unstable endoperoxide and an electronically excited 3-APA* anion, leading to light emission. The $O_2^{\bullet-}$ radical is probably formed by oxygen reduction by sulfite in an alkaline solution. The $^{\bullet}OH$ radical is probably generated from the reaction between ferrous iron (from Fe^{3+} reduction by sulfite) with molecular oxygen.

In our case, at low sulfite concentration levels, CL inhibition of the luminol–$CoFe_2O_4$ NP–sulfite system occurs. This can be tentatively explained by the dissolved oxygen consumption by sulfite. According to Contreras,[63] the dissolved oxygen consumption in the presence of a low sulfite concentration level

dx.doi.org/10.1021/jf3041269 | J. Agric. Food Chem. 2013, 61, 840–847

Table 2. Recoveries of Sulfite in the Presence of Foreign Species (Sulfite Concentration 1.0×10^{-5} M)

coexisting species	concn (mg L^{-1})	recovery[a] (%)	coexisting species	concn (μg L^{-1})	recovery[a] (%)
Na^+	23	101.25 ± 2.99	Pb^{2+}	1000	104.95 ± 1.34
K^+	39	102.57 ± 1.31	Al^{3+}	135	97.47 ± 1.01
Ca^{2+}	40	99.30 ± 3.63	Zn^{2+}	325	95.87 ± 1.66
Mg^{2+}	24	98.16 ± 2.89	Ni^{2+}	295	104.20 ± 1.20
HPO_4^{2-}	96	96.18 ± 0.61	Co^{2+}	59	104.43 ± 2.38
Cl^-	36	102.57 ± 1.31	Fe^{3+}	56	212.72 ± 1.30
NH_4^+	42	104.83 ± 2.30	Cu^{2+}	64	50.92 ± 4.54
$H_2PO_4^-$	97	97.52 ± 1.38	Fe^{3+}–EDTA[b]	56	95.31 ± 1.57
SO_4^{2-}	98	95.89 ± 2.45	Cu^{2+}–EDTA[b]	64	93.90 ± 0.30
NO_3^-	62	107.59 ± 2.71			

[a]Mean value ± standard deviation (n = 3). [b]EDTA concentration 1.0×10^{-6} M.

Table 3. Determination Results (mg L^{-1}) of Sulfite in White Wine Samples

sample	proposed method[a]	titration method[a]
white wine 1	97.2 ± 1.1	103.5 ± 2.9
white wine 2	146.5 ± 0.5	130.6 ± 2.2
white wine 3	82.4 ± 1.4	99.3 ± 2.5
white wine 4	110.6 ± 0.5	121.8 ± 1.1

[a]Average of three measurements (±RSD%).

may be the main controlling factor for the studied system, leading to a decrease of the CL response. At high sulfite concentration levels, CL enhancement of the luminol–$CoFe_2O_4$ NP–sulfite system occurs. This can be tentatively explained by the most accepted radical mechanism for sulfite oxidation by dissolved oxygen. The sulfite oxidation by dissolved oxygen takes place through complex chain reactions involving radicals such as $SO_3^{\bullet-}$, $SO_4^{\bullet-}$, $SO_5^{\bullet-}$, and $^{\bullet}OH$.[64,65] It is well-known that a dilute solution of sulfite undergoes autoxidation,[16,17,66,67] which would produce $SO_3^{\bullet}$ free radical.[17] Also, Fe^{3+} adsorbed on the surface of $CoFe_2O_4$ NPs reacts with sulfite to produce $SO_3^{\bullet-}$ radical, followed by a propagation reaction to produce stronger oxidative radicals such as $SO_5^{\bullet-}$ and $SO_4^{\bullet-}$.[63] In addition, the one-electron reduction of $SO_5^{\bullet-}$ yields HSO_5^-, which could react with Fe^{2+} to generate $^{\bullet}OH$ radical and $SO_4^{\bullet-}$ radical.[65] These produced stronger oxidative radicals could react with luminol to produce the intensified CL response. As a result, the CL emission was enhanced.

In summary, $CoFe_2O_4$ NPs were found to possess intrinsic oxidase-like activity and could catalytically oxidize TMB, OPD, and ABTS by dissolved O_2 to produce a color reaction. As an oxidase mimic, the $CoFe_2O_4$ NPs could catalyze luminol oxidation by dissolved oxygen to produce intensified CL. An investigation on the effect of sulfite on $CoFe_2O_4$ NP oxidase mimic-mediated CL of aqueous luminol demonstrates that the CL enhancement and inhibition of the luminol–$CoFe_2O_4$ NP–sulfite system depend on the sulfite concentration and solution pH. The results of the kinetic curves and the CL spectra of the studied system suggest that addition of $CoFe_2O_4$ NPs or sulfite into a luminol solution does not produce a new luminophore of the chemiluminescent reaction. On this basis, a new flow injection CL assay to detect sulfite was constructed and has been applied to the determination of trace sulfite in white wine samples with satisfactory results.

■ ASSOCIATED CONTENT

Ⓢ Supporting Information

Effect of the $CoFe_2O_4$ NP concentration and luminol concentration on kinetic curves of the reaction system and effect of TPA and BQ on CL responses of aqueous luminol–$CoFe_2O_4$ NP systems with and without 1.0×10^{-3} or 5.0×10^{-5} M sulfite. This material is available free of charge via the Internet at http://pubs.acs.org.

■ AUTHOR INFORMATION

Corresponding Author

*Phone/fax: +86 23 38254346 (Z.C.); +86 23 68254843 (Y.H.). E-mail: zhaohuic@swu.edu.cn (Z.C.); yuminghuang2000@yahoo.com (Y.H.).

Funding

Financial support from the National Natural Science Foundation of China (Grant 21075099) and State Key Laboratory Breeding Base of Eco-Environments and Bio-Resources of the Three Gorges Reservoir Region (Grant SKL-2011-08) is gratefully acknowledged.

Notes

The authors declare no competing financial interest.

■ REFERENCES

(1) Gunnison, A. F.; Jacobsen, D. W. Sulfite hypersensitivity. A critical review. *CRC Crit. Rev. Toxicol.* **1987**, *17*, 185–214.
(2) Simon, R. A. Sulfite sensitivity. *Ann. Allergy* **1986**, *56*, 281–288.
(3) Küçükatay, V.; Savcıoğlu, F.; Hacıoğlu, G.; Yargıçoğlu, P.; Ağar, A. Effect of sulfite on cognitive function in normal and sulfite oxidase deficient rats. *Neurotoxicol. Teratol.* **2005**, *27*, 47–54.
(4) Kodavanti, U. P.; Mebane, R.; Ledbetter, A.; Krantz, T.; McGee, J.; Jackson, M. C.; Walsh, L.; Hilliard, H.; Chen, B. Y.; Richards, J.; Costa, D. L. Variable pulmonary responses from exposure to concentrated ambient air particles in a rat model of bronchitis. *Toxicol. Sci.* **2000**, *54*, 441–451.
(5) Samet, J. M.; Dominici, F.; Curriero, F. C.; Coursac, I.; Zeger, S. L. Variable pulmonary responses from exposure to concentrated ambient air particles in a rat model of bronchitis. Fine particulate air pollution and mortality in 20 U.S. cities, 1987–1994. *N. Engl. J. Med.* **2000**, *343*, 1742–1749.
(6) Allen, D. H. Asthma induced by sulphites. *Food Technol. Aust.* **1985**, *73*, 506–509.
(7) Lawrence, J. F.; Chadha, R. K. Determination of sulfite in foods by headspace liquid chromatography. *J.—Assoc. Off. Anal. Chem.* **1988**, *71*, 930–933.
(8) Ohira, S. I.; Toda, K. Ion chromatographic measurement of sulfide, methanethiolate, sulfite and sulfate in aqueous and air samples. *J. Chromatogr., A* **2006**, *1121*, 280–284.

(9) Masár, M.; Danková, M.; Ölvecká, E.; Stachurová, A.; Kaniansky, D.; Stanislawski, B. Determination of free sulfite in wine by zone electrophoresis with isotachophoresis sample pretreatment on a column-coupling chip. *J. Chromatogr., A* **2004**, *1026*, 31−39.
(10) Alamo, L. S. T.; Tangkuaram, T.; Satienperakul, S. Determination of sulfite by pervaporation-flow injection with amperometric detection using copper hexacyanoferrate-carbon nanotube modified carbon paste electrode. *Talanta* **2010**, *81*, 1793−1799.
(11) Zhao, M.; Hibbert, D. B.; Gooding, J. J. Determination of sulfite in beer samples using an amperometric fill and flow channel biosensor employing sulfite oxidase. *Anal. Chim. Acta* **2006**, *556*, 195−200.
(12) Sezgintürk, M. K.; Dinçkaya, E. Direct determination of sulfite in food samples by a biosensor based on plant tissue homogenate. *Talanta* **2005**, *65*, 998−1002.
(13) Spricigo, R.; Dronov, R.; Lisdat, F.; Leimkühler, S.; Scheller, F. W.; Wollenberger, U. Electrocatalytic sulfite biosensor with human sulfite oxidase co-immobilized with cytochrome c in a polyelectrolyte-containing multilayer. *Anal. Bioanal. Chem.* **2009**, *393*, 225−233.
(14) Hassan, S. S. M.; Hamza, M. S. A.; Mohamed, A. H. K. A novel spectrophotometric method for batch and flow injection determination of sulfite in beverages. *Anal. Chim. Acta* **2006**, *570*, 232−239.
(15) Yamada, M.; Nakada, T.; Suzuki, S. The determination of sulfite in a flow injection system with chemiluminescence detection. *Anal. Chim. Acta* **1983**, *147*, 401−404.
(16) Al-Tamrah, S. A.; Townshend, A.; Wheatley, A. R. Flow injection chemiluminescence determination of sulphite. *Analyst* **1987**, *112*, 883−886.
(17) Huang, Y.; Zhang, C.; Zhang, X.; Zhang, Z. Chemiluminescence of sulfite based on auto-oxidation sensitized by rhodamine 6G. *Anal. Chim. Acta* **1999**, *391*, 95−100.
(18) Bonifácio, R. L.; Coichev, N. Chemiluminescent determination of sulfite traces based on the induced oxidation of Ni(II)/tetraglycine complex by oxygen in the presence of luminol: Mechanistic considerations. *Anal. Chim. Acta* **2004**, *517*, 125−130.
(19) Sun, C.; Liu, B.; Li, J. Sensitized chemiluminescence of CdTe quantum-dots on Ce(IV)-sulfite and its analytical applications. *Talanta* **2008**, *75*, 447−454.
(20) Adcock, J. L.; Francis, P. S.; Barnett, N. W. Acidic potassium permanganate as a chemiluminescence reagent. *Anal. Chim. Acta* **2007**, *601*, 36−67.
(21) Gorman, B. A.; Francis, P. S.; Barnett, N. W. Tris(2,2′-bipyridyl) ruthenium(II) chemiluminescence. *Analyst* **2006**, *131*, 616−639.
(22) Marquette, C. A.; Blum, L. J. Applications of the luminol chemiluminescent reaction in analytical chemistry. *Anal. Bioanal. Chem.* **2006**, *385*, 546−554.
(23) Liu, G. H.; Zhu, Y. F.; Zhang, X. R.; Xu, B. Q. Chemiluminescence determination of chlorinated volatile organic compounds by conversion on nanometer TiO_2. *Anal. Chem.* **2002**, *74*, 6279−6284.
(24) Zhu, Y. F.; Shi, J. J.; Zhang, Z. Y.; Zhang, C.; Zhang, X. R. Development of a gas sensor utilizing chemiluminescence on nanosized titanium dioxide. *Anal. Chem.* **2002**, *74*, 120−124.
(25) Cui, H.; Zhang, Z. F.; Shi, M. J.; Xu, Y.; Wu, Y. L. Light emission of gold nanoparticles induced by the reaction of bis(2,4,6-trichlorophenyl) oxalate and hydrogen peroxide. *Anal. Chem.* **2005**, *77*, 6402−6406.
(26) Zhang, Z. F.; Cui, H.; Lai, C. Z.; Liu, L. J. Gold nanoparticles-catalyzed luminol chemiluminescence and its analytical applications. *Anal. Chem.* **2005**, *77*, 3324−3329.
(27) Zhang, Z. F.; Cui, H.; Shi, M. J. Chemiluminescence accompanied by the reaction of gold nanoparticles with potassium permanganate. *Phys. Chem. Chem. Phys.* **2006**, *8*, 1017−1021.
(28) Bi, S.; Yan, Y.; Yang, X.; Zhang, S. Gold nanolabels for new enhanced chemiluminescence immunoassay of alpha-fetoprotein based on magnetic beads. *Chem.—Eur. J.* **2009**, *15*, 4704−4709.
(29) Li, S. F.; Zhang, X. M.; Du, W. X.; Ni, Y. H.; Wei, X. W. Chemiluminescence reactions of a luminol system catalyzed by ZnO nanoparticles. *J. Phys. Chem. C* **2009**, *113*, 1046−1051.
(30) Lin, J. M.; Liu, M. L. Chemiluminescence from the decomposition of peroxymonocarbonate catalyzed by gold nanoparticles. *J. Phys. Chem. B* **2008**, *112*, 7850−7855.
(31) Niazov, T.; Shlyahovsky, B.; Willner, I. Photoswitchable electrocatalysis and catalyzed chemiluminescence using photoisomerizable monolayer-functionalized surfaces and Pt nanoparticles. *J. Am. Chem. Soc.* **2007**, *129*, 6374−6375.
(32) Poznyak, S. K.; Talapin, D. V.; Shevchenko, E. V.; Weller, H. Quantum dot chemiluminescence. *Nano Lett.* **2004**, *4*, 693−698.
(33) Liu, D.; Liu, M. Y.; Liu, G. H.; Zhang, S. C.; Wu, Y. Y.; Zhang, X. R. Dual-channel sensing of volatile organic compounds with semiconducting nanoparticles. *Anal. Chem.* **2010**, *82*, 66−68.
(34) Cho, S. J.; Idrobo, J. C.; Olamit, J.; Liu, K.; Browning, N. D.; Kauzlarich, S. M. Growth mechanisms and oxidation-resistance of gold-coated iron nanoparticles. *Chem. Mater.* **2005**, *17*, 3181−3186.
(35) Gao, L. Z.; Zhuang, J.; Nie, L.; Zhang, J. B.; Zhang, Y.; Gu, N.; Wang, T. H.; Feng, J.; Yang, D. L.; Perrett, S.; Yan, X. Y. Intrinsic peroxidase-like activity of ferromagnetic nanoparticles. *Nat. Nanotechnol.* **2007**, *2*, 577−583.
(36) Wei, H.; Wang, E. Fe_3O_4 magnetic nanoparticles as peroxidase mimetics and their applications in H_2O_2 and glucose detection. *Anal. Chem.* **2008**, *80*, 2250−2254.
(37) Fang, Y.; Huang, Y. The effective peroxidase-like activity of chitosan-functionalized $CoFe_2O_4$ nanoparticles for chemiluminescence sensing of hydrogen peroxide and glucose. *Analyst* **2012**, *137*, 1225−1231.
(38) Shi, W.; Zhang, X.; He, S.; Huang, Y. $CoFe_2O_4$ magnetic nanoparticles as a peroxidase mimic mediated chemiluminescence for hydrogen peroxide and glucose. *Chem. Commun.* **2011**, *47*, 10785−10787.
(39) Yu, F.; Huang, Y.; Cole, A. J.; Yang, V. C. The artificial peroxidase activity of magnetic iron oxide nanoparticles and its application to glucose detection. *Biomaterials* **2009**, *30*, 4716−4722.
(40) Liu, S.; Lu, F.; Xing, R.; Zhu, J. J. Structural effects of Fe_3O_4 nanocrystals on peroxidase-like activity. *Chem.—Eur. J.* **2011**, *17*, 620−625.
(41) André, R.; Natálio, F.; Humanes, M.; Leppin, J.; Heinze, K.; Wever, R.; Schröder, H. C.; Müller, W. E. G.; Tremel, W. V_2O_5 nanowires with an intrinsic peroxidase-like activity. *Adv. Funct. Mater.* **2011**, *21*, 501−509.
(42) Korsvik, C.; Patil, S.; Seal, S.; Self, W. T. Superoxide dismutase mimetic properties exhibited by vacancy engineered ceria nanoparticles. *Chem. Commun.* **2007**, *10*, 1056−1058.
(43) Asati, A.; Santra, S.; Kaittanis, C.; Nath, S.; Perez, J. M. Oxidase activity of polymer-coated cerium oxide nanoparticles. *Angew. Chem., Int. Ed.* **2009**, *48*, 2308−2312.
(44) Pirmohamed, T.; Dowding, J. M.; Singh, S.; Wasserman, B.; Heckert, E.; Karakoti, A. S.; King, J. E. S.; Seal, S.; Self, W. T. Nanoceria exhibit redox state-dependent catalase mimetic activity. *Chem. Commun.* **2010**, *46*, 2736−2738.
(45) Jv, Y.; Li, B.; Cao, R. Positively-charged gold nanoparticles as peroxidiase mimic and their application in hydrogen peroxide and glucose detection. *Chem. Commun.* **2010**, *46*, 8017−8019.
(46) Fan, J.; Yin, J. J.; Ning, B.; Wu, X.; Hu, Y.; Ferrari, M.; Anderson, G. J.; Wei, J.; Zhao, Y.; Nie, G. Direct evidence for catalase and peroxidase activities of ferritin-platinum nanoparticles. *Biomaterials* **2011**, *32*, 1611−1618.
(47) He, W.; Liu, Y.; Yuan, J.; Yin, J. J.; Wu, X.; Hu, X.; Zhang, K.; Liu, J.; Chen, C.; Ji, Y.; Guo, Y. Au@Pt nanostructures as oxidase and peroxidase mimetics for use in immunoassays. *Biomaterials* **2011**, *32*, 1139−1147.
(48) Liu, J.; Hu, X.; Hou, S.; Wen, T.; Liu, W.; Zhu, X.; Wu, X. Screening of inhibitors for oxidase mimics of Au@Pt nanorods by catalytic oxidation of OPD. *Chem. Commun.* **2011**, *47*, 10981−10983.
(49) Wang, X. X.; Wu, Q.; Shan, Z.; Huang, Q. M. BSA-stabilized Au clusters as peroxidase mimetics for use in xanthine detection. *Biosens. Bioelectron.* **2011**, *26*, 3614−3619.

(50) Song, Y.; Qu, K.; Zhao, C.; Ren, J.; Qu, X. Graphene oxide: Intrinsic peroxidase catalytic activity and its application to glucose detection. *Adv. Mater.* **2010**, *22*, 2206−2210.
(51) Song, Y.; Wang, X.; Zhao, C.; Qu, K.; Ren, J.; Qu, X. Label-free colorimetric detection of single nucleotide polymorphism by using single-walled carbon nanotube intrinsic peroxidase-like activity. *Chem.—Eur. J.* **2010**, *16*, 3617−3621.
(52) Shi, W.; Wang, Q.; Long, Y.; Cheng, Z.; Chen, S.; Zheng, H.; Huang, Y. Carbon nanodots as peroxidase mimetics and their applications to glucose detection. *Chem. Commun.* **2011**, *47*, 6695−6697.
(53) Song, Y.; Chen, Y.; Feng, L.; Qu, X. Selective and quantitative cancer cell detection using target-directed functionalized graphene and its synergetic peroxidase-like activity. *Chem. Commun.* **2011**, *47*, 4436−4438.
(54) Wang, X.; Qu, K.; Xu, B.; Ren, J.; Qu, X. Multicolor luminescent carbon nanoparticles: Synthesis, supramolecular assembly with porphyrin, intrinsic peroxidase-like catalytic activity and applications. *Nano Res.* **2011**, *4*, 908−920.
(55) Song, Y.; Wei, W.; Qu, X. Colorimetric biosensing using smart materials. *Adv. Mater.* **2011**, *23*, 4215−4236.
(56) Xie, J.; Zhang, X.; Wang, H.; Zheng, H.; Huang, Y. Analytical and environmental applications of nanoparticles as enzyme mimetics. *TrAC, Trends Anal. Chem.* **2012**, *30*, 114−129.
(57) *State Standard of the People's Republic of China—Method for Determination of Sulfites in Foods*; GB/T 5009.34-1996; Standards Press of China: Beijing, 1996.
(58) Merényi, G.; Lind, J.; Eriksen, T. E. Luminol chemiluminescence: Chemistry, excitation, emitter. *J. Biolumin. Chemilumin.* **1990**, *5*, 53−56.
(59) Faulkner, K.; Fridovich, I. Luminol and lucigenin as detectors for $O_2^{\bullet -}$. *J. Free Radical Biol. Med.* **1993**, *15*, 447−451.
(60) Manring, L. E.; Kramer, M. K.; Foote, C. S. Interception of O_2^- by benzoquinone in cyanoaromatic-sensitized photooxygenations. *Tetrahedron Lett.* **1984**, *25*, 2523−2526.
(61) Hayon, E.; Simic, M. Acid-base properties of free radicals in solution. *Acc. Chem. Res.* **1974**, *7*, 114−121.
(62) Ishibasi, K.; Fujishima, A.; Watanabe, T.; Hashimoto, K. Quantum yields of active oxidative species formed on TiO_2 photocatalyst. *J. Photochem. Photobiol., A* **2000**, *134*, 139−142.
(63) Contreras, E. M. Stoichiometry of sulfite oxidation by oxygen during the determination of the volumetric mass transfer coefficient. *Ind. Eng. Chem. Res.* **2008**, *47*, 9709−9714.
(64) Lancia, A.; Musmarra, D.; Pepe, F.; Prisciandaro, M. Model of oxygen absorption into calcium sulfite solutions. *Chem. Eng. J.* **1997**, *66*, 123−129.
(65) Netta, P.; Huie, R. E. Free-radical chemistry of sulfite. *Environ. Health Perspect.* **1985**, *64*, 209−217.
(66) Paulls, D. A.; Townshend, A. Enhancement by cycloalkanes of the chemiluminescent oxidation of sulfite. *Analyst* **1996**, *121*, 831−834.
(67) Paulls, D. A.; Townshend, A. Sensitized determination of sulfite using flow injection with chemiluminescent detection. *Analyst* **1995**, *120*, 467−469.